Journal of Asian Ceramic Societies 4 (2016) 209–218

Contents lists available at ScienceDirect

Journal of Asian Ceramic Societies

journal homepage: www.elsevier.com/locate/jascer

Influence of ceramic particulate type on microstructure and tensile strength of aluminum matrix composites produced using friction stir processing

I. Dinaharan*

Department of Mechanical Engineering Science, University of Johannesburg, Auckland Park Kingsway Campus, Johannesburg 2006, South Africa

ARTICLE INFO

Article history:
Received 8 February 2016
Received in revised form 28 March 2016
Accepted 13 April 2016
Available online 29 April 2016

Keywords:
Aluminum matrix composites
Friction stir processing
Microstructure
Tensile strength

ABSTRACT

Friction stir processing (FSP) was applied to produce aluminum matrix composites (AMCs). Aluminum alloy AA6082 was used as the matrix material. Various ceramic particles, such as SiC, Al_2O_3, TiC, B_4C and WC, were used as reinforcement particle. AA6082 AMCs were produced using a set of optimized process parameters. The microstructure was studied using optical microscopy, filed emission scanning electron microscopy and electron back scattered diagram. The results indicated that the type of ceramic particle did not considerably vary the microstructure and ultimate tensile strength (UTS). Each type of ceramic particle provided a homogeneous dispersion in the stir zone irrespective of the location and good interfacial bonding. Nevertheless, AA6082/TiC AMC exhibited superior hardness and wear resistance compared to other AMCs produced in this work under the same set of experimental conditions. The strengthening mechanisms and the variation in the properties are correlated to the observed microstructure. The details of fracture mode are further presented.

1. Introduction

Reinforcing aluminum alloys with ceramic particles creates high elastic modulus, stiffness and wear resistance. The resultant material is universally called as aluminum matrix composites (AMCs). The research on AMCs is intensified due to the great interest of the automobile, aerospace and defense industries to replace conventional aluminum alloys in several applications [1–3]. The performance and properties of the AMCs depend on several aspects, which are not limited to uniform distribution of reinforcing particles, interfacial bonding between the aluminum matrix and the reinforcing particles and integrity of the reinforcing particle during the production process [4]. Therefore, it is an uphill task to produce sound AMCs showcasing uniform distribution and good interfacial bonding without decomposing of reinforcing particles. Hitherto, powder metallurgy and stir casting were predominantly used to produce AMCs. But, the common defects, such as porosity, clustering and segregation of particles and interfacial reactions, are always encountered [5–9].

Friction stir processing (FSP) has emerged as a potential solid-state technique to produce sound AMCs. It is facile and economic to prepare AMCs using FSP. The ceramic particles are compacted initially along the FSP direction using grooves of various shapes. A square groove is preferred to compact particles. The open end of the groove is closed by traversing a pinless tool prior to FSP to avoid the loss of ceramic particles during processing. The frictional heat generated by the rotating shoulder and the pin helps to plasticize the aluminum alloy. The transverse movement of the tool results in the transportation of plasticized material from the advancing side to the retreading side. Subsequently, the groove portion collapses and the stirring action of the tool disperses the packed ceramic particles into the plasticized aluminum alloy. The AMCs are thus formed and forged at the back of the tool due to the applied axial force. FSP is a low energy consumption process. The entire process is accomplished in solid state without melting of aluminum. Hence, the chances of interfacial reaction and decomposition are remote. Neither the density gradient between the ceramic particle and the aluminum alloy nor the particle size influences the ultimate distribution of particles [10–13].

AMCs reinforced with varieties of ceramic particles produced using FSP were reported in literatures [14–22]. Shahraki et al.

* Tel.: +27 797018997.
E-mail address: dinaweld2009@gmail.com
Peer review under responsibility of The Ceramic Society of Japan and the Korean Ceramic Society.

http://dx.doi.org/10.1016/j.jascer.2016.04.002

Table 1
Chemical composition of AA6082 aluminum alloy.

Element	Mg	Si	Fe	Mn	Cu	Cr	Zn	Ti	Aluminum
wt.%	0.78	1.06	0.21	0.55	0.09	0.03	0.06	0.01	Balance

[14] developed AA5083/ZrO_2 AMCs and evaluated the microstructure and tensile behavior. Moghaddas and Bozorg [15] produced AA5754/Si_3N_4 AMCs and correlated the thermal profiles with the evolution of microstructure. You et al. [16] prepared Al/SiO_2 AMCs and analysed the in situ formation of Al_2O_3 particles. Bahrami et al. [17] fabricated AA7075/SiC AMCs and analyzed the role of tool pin geometry on microstructure and mechanical properties. Mazaheri et al. [18] synthesized A356/Al_2O_3 AMCs and investigated the microstructure and tribological behavior. Khodabakhshi et al. [19] created AA5052/TiO_2 AMCs and studied the effect of annealing on the soild-state chemical reactions. Thangarasu et al. [20] produced AA6082/TiC AMCs and examined the effect of TiC content on microstructure and tensile strength. Zhao et al. [21] prepared AA6061/B_4C AMCs and studied the effect of number of passes on the distribution of B_4C particles. Hashemi and Hussain [22] formed AA7075/TiN AMCs and estimated the influence of tool design on dry sliding wear behavior.

It is inferred from the short literature survey that FSP has been successfully applied to produce AMCs reinforced with various ceramic particulates, including SiC, Al_2O_3, B_4C, TiC, ZrO_2, Si_3N_4, SiO_2, TiO_2 and TiN. However, various ceramic particles were not compared in any single research work, which would assist to assess the performance of several potential reinforcements under a set of identical experimental conditions. Therefore, the objective of this research work is to produce AMCs reinforced with SiC, Al_2O_3, TiC, B_4C and WC and evaluate the effect of various reinforcements on the microstructure and tensile behavior.

2. Experimental procedure

Aluminum alloy AA6082 plates of size 100 mm × 50 mm × 10 mm were used for this research work. The chemical composition of AA6082 aluminum alloy is furnished in Table 1. A groove of 5 mm deep and 1.2 width was machined along the center line of the plates

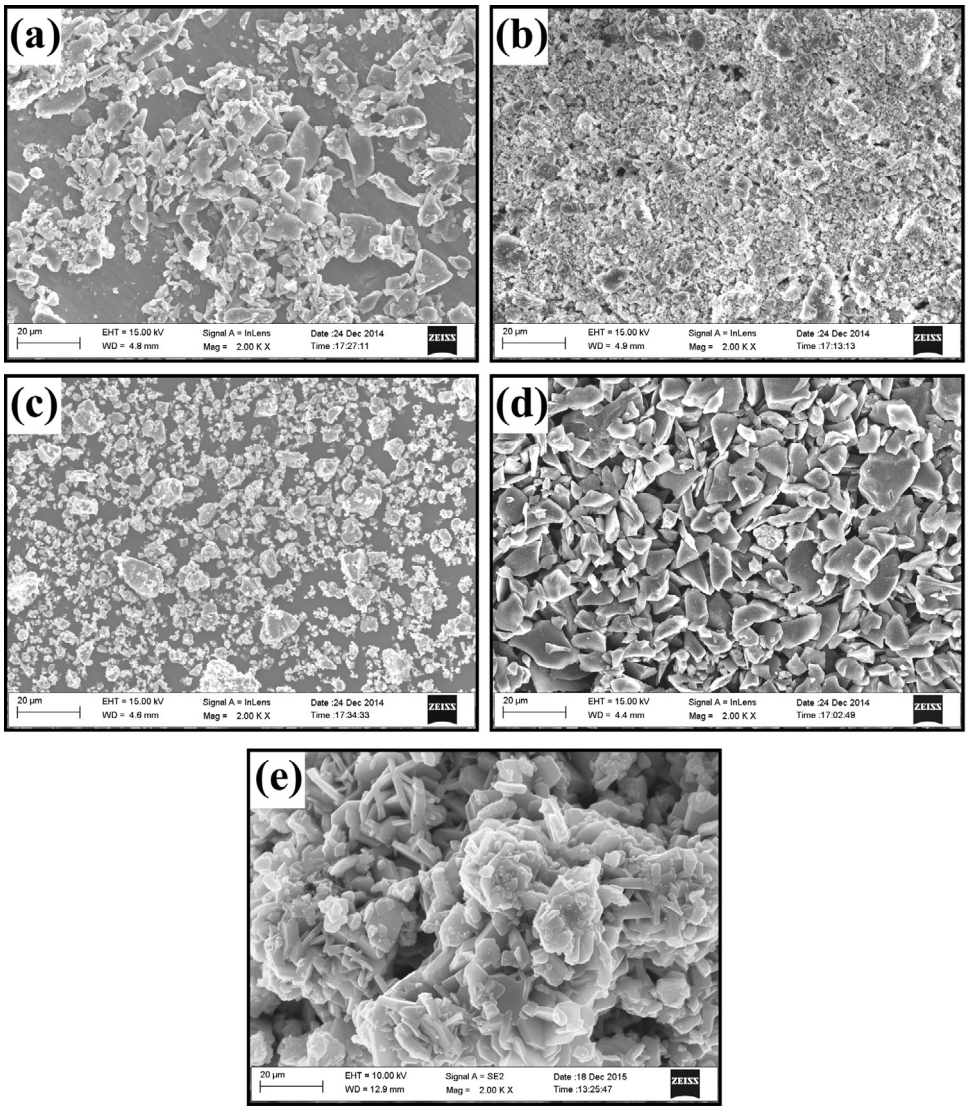

Fig. 1. FESEM micrograph of ceramic particles; (a) SiC, (b) Al_2O_3, (c) TiC, (d) B_4C and (e) WC.

using wire cut Electrical Discharge Machining (EDM). The volume fraction of ceramic particle was 18%. The SEM micrographs of as-received ceramic particles are shown in Fig. 1. A pinless tool was initially employed to cover the top of the groove after filling with ceramic particles to prevent the particles from scattering during FSP. The FSP was carried out on an indigenously built FSW machine. The tool had a shoulder diameter of 18 mm, pin diameter of 5 mm, pin length of 5.5 mm and a threaded pin profile. The tool material was high carbon high chromium steel (HCHCr), which was oil hardened to obtain a hardness of 60–62 HRC. The process parameters employed were tool rotational speed of 1600 rpm, travel speed of 60 mm/min and axial force of 10 kN. The parameters were selected based on trial experiments and previous works done by the author. Five such plates were friction stir processed by varying ceramic particles, such as SiC (~8 μm), Al_2O_3 (~1 μm), TiC (~2 μm), B_4C (~4 μm) and WC (~5 μm). A detailed FSP procedure to produce the composite is presented elsewhere [23].

Specimens were obtained from the center of the friction stir processed plates and were polished as per standard metallographic procedure. The polished specimens were etched with Keller's reagent. The microstructure was observed using an optical microscope (OLYMPUS-BX51M) at various locations in the stir zone. The ceramic particle distribution was further viewed using a field emission scanning electron microscope (FESEM, CARL ZEISS-SIGMA HV) and electron backscatter diffraction (EBSD). An acceleration voltage of 15 kV was selected for FESEM. EBSD was carried out in a FEI Quanta FEG SEM equipped with TSL-OIM software. The mean grain size was measured according to ASTM E1382–97. The microhardness was measured using a microhardness tester (MITUTOYO-MVK-H1) at 500 g load applied for 15 s at various locations in the surface composite. Mini tensile specimens of gauge length 21 mm and diameter 4 mm were prepared as per ASTM B557M-10 standard from the FSP zone. The ultimate tensile strength (UTS) was estimated using a computerized tensile tester. The fracture surfaces were viewed using SEM.

3. Results and discussion

3.1. Microstructure of AA6082 AMCs

Fig. 2 shows representative SEM micrographs of AA6082 AMCs reinforced with various ceramic particles, which clearly reveal the dispersion of ceramic particles in the aluminum matrix. The dispersion of ceramic particles is observed to be fairly homogeneous. There are no clusters or agglomeration of particles seen. Moreover, there is no segregation of particles along the grain boundaries.

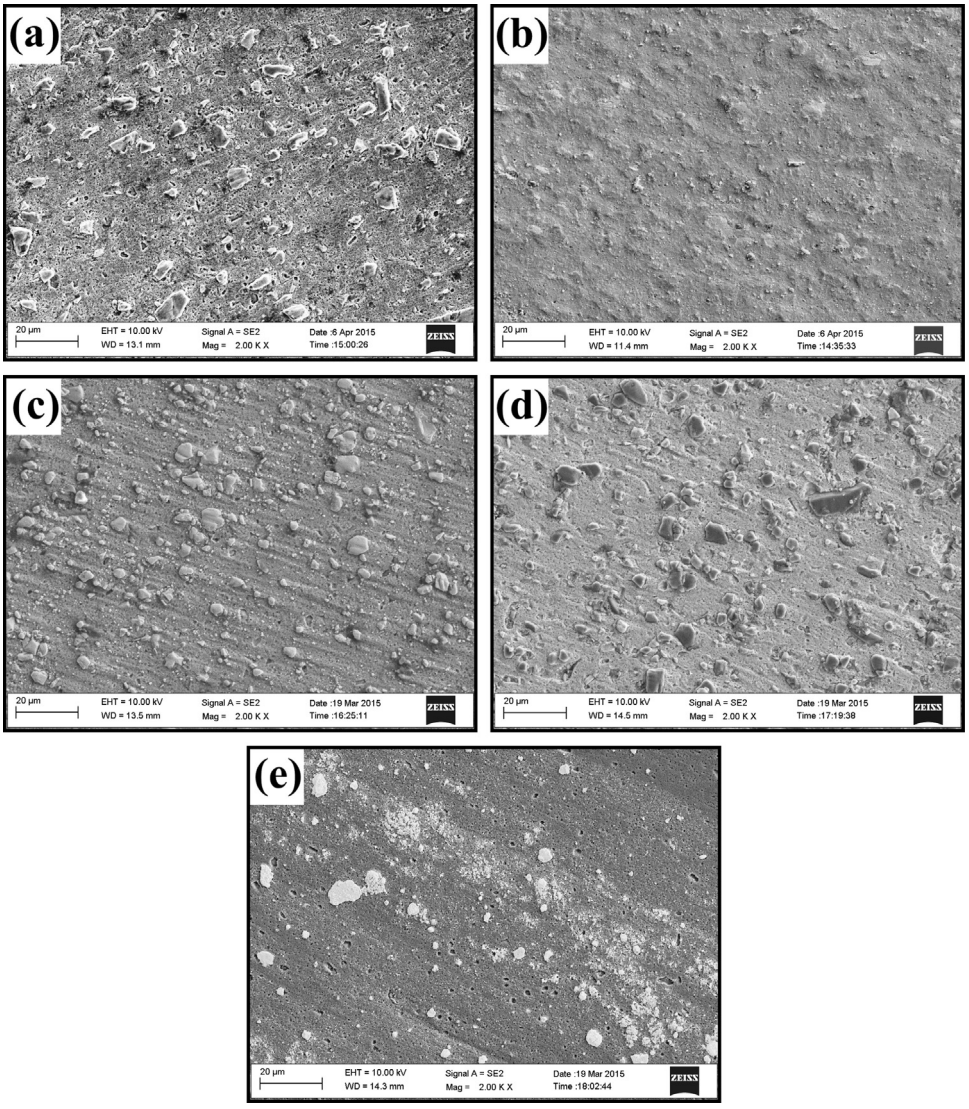

Fig. 2. FESEM micrograph AA6082 AMCs reinforced with (a) SiC, (b) Al_2O_3, (c) TiC, (d) B_4C and (e) WC.

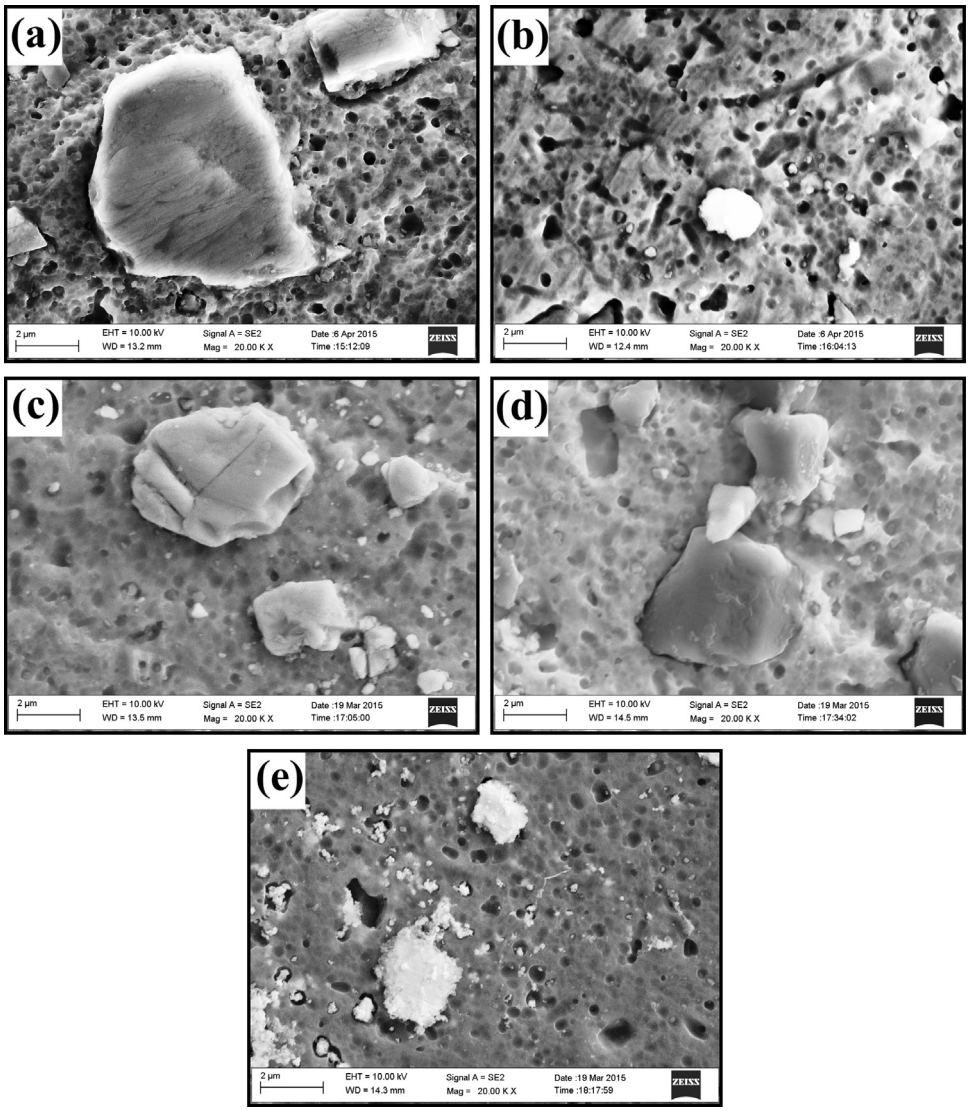

Fig. 3. FESEM micrograph AA6082 AMCs reinforced with (a) SiC, (b) Al_2O_3, (c) TiC, (d) B_4C and (e) WC at higher magnification.

Some particles might be located on the grain boundaries due to smaller grain size. But entrapment of particles within grain boundaries is absent. Hence, the dispersion is considered to be roughly intragranular. The mechanical and tribological properties of AMCs are influenced by the nature of dispersion. A homogeneous and intragranular dispersion is essential to attain higher properties. The FSP process has resulted in the desirable dispersion. Stir casting technique frequently produces inhomogeneous and intergranular dispersion owing to solidification related phenomena. The density gradient results in improper dispersion [8]. Since the aluminum matrix does not melt during FSP, density gradient does not cause free movement of ceramic particles. This leads to proper dispersion. The dispersion of ceramic particles is a function of process parameters, such as tool rotational speed and traverse speed [12,13,15,24]. A fine and homogeneous dispersion in the SEM micrographs confirm that the chosen set of process parameters is sufficient to produce the desirable dispersion. The compacted ceramic particles are dispersed throughout the stir zone.

FSP induced a change in the size and morphology of ceramic particles, Figs. 1 and 2. The severe plastic deformation together with the rotating action of the tool is able to smash the ceramic particles. The strong stirring action of the tool knocks off the sharp corners of the ceramic particle. Large size variation of ceramic particles (SiC, TiC, B_4C and WC) in Fig. 2 indicates the fragmentation. Similar observations were reported by other researchers [13,25]. The rate of fragmentation depends upon the initial size and shape of the particles. Large size particles and irregular or polygonal shape particles have the tendency to break off during FSP. The retention of shape and size of Al_2O_3 particles in Fig. 2 after FSP, which did not undergo much fragmentation, confirms this statement. It is observed in Fig. 2 that the large ceramic particles are not surrounded by debris generated due to fragmentation. There is no clustering of small debris either. This suggests that the debris also mixed well with the plasticized aluminum and dispersed homogeneously in the AMC. The size of debris is remarkably low in the order of nanometer compared to the size of initially packed ceramic particles. The size variation leads to functionally graded local areas within the AMC.

Fig. 3 presents the SEM micrographs of AA6082 AMCs reinforced with various ceramic particles at higher magnification. The interface between the aluminum matrix and the ceramic particle is detailed in this figure. The interface is clear without the presence of pores or reaction products. Each type of ceramic particle appears to be bonded well with the aluminum matrix. Some investigators observed pores around ceramic particles in AMCS produced using FSP [12,13]. No such pores are observed near any ceramic particle in Fig. 3. This can be attributed to adequate material flow and

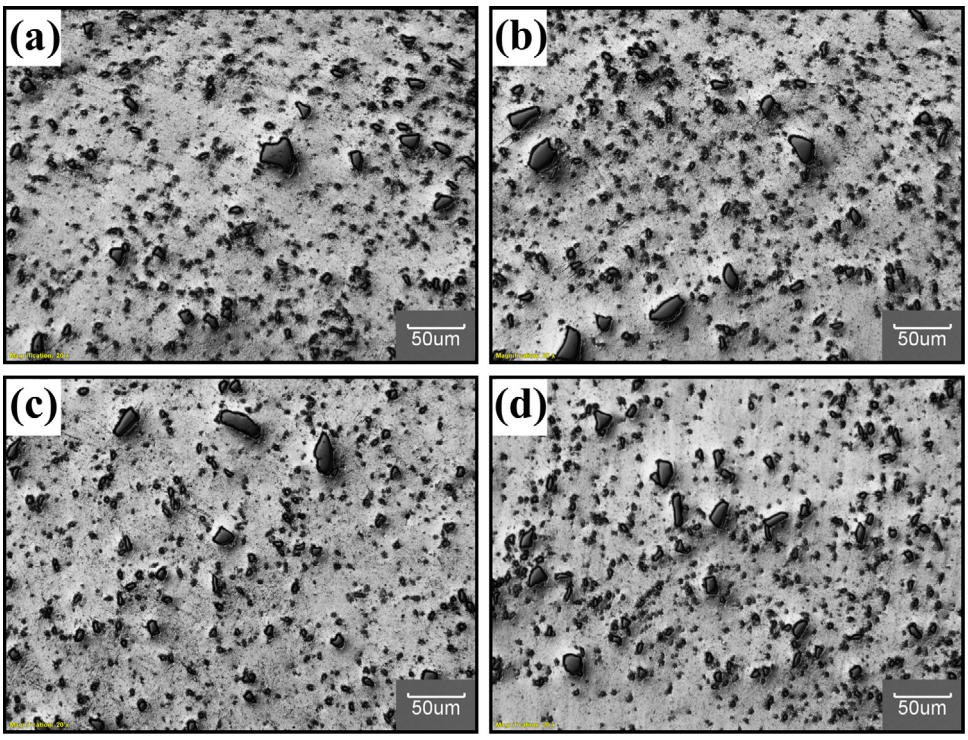

Fig. 4. Optical photomicrograph of AA6082/SiC AMCs observed at various locations within the stir zone; (a) near advancing side, (b) near retreading side; (c) center and (d) bottom.

plasticization of aluminum under the chosen experimental conditions. The interface plays a crucial role in tensile loading to transfer the load effectively to the ceramic particle. Good interfacial bonding is a prerequisite in spite of homogeneous dispersion to improve the properties. The temperature of the processing method influences the interfacial strength significantly. Higher processing temperature tends to initiate interfacial reactions between the aluminum matrix and the ceramic particle. The reaction products usually surround the ceramic particle and weaken the interfacial strength [8]. Absence of reaction products indicates that the temperature rise during FSP is insufficient to initiate any interfacial reaction.

Figs. 4–8 presents the optical micrographs of AA6082 AMCs reinforced with various ceramic particles captured at different locations within the stir zone. The optical micrographs show the dispersion of ceramic particles all over the stir zone. No area in the stir zone is left without particles. It is significant to observe that the dispersion of the ceramic particle is independent of the location in the stir zone. The change in the dispersion of the ceramic particles from the advancing side to the retreading side or from the top side to the bottom side is negligible. However, some researchers found significant variation in the distribution of ceramic particles within the stir zone of AMCs produced by FSP [14,26,27].

The absence of significant variation in dispersion can be ascribed to adequate plasticization of aluminum matrix and optimized tool rotational speed, which makes easy to disperse the ceramic particles to all regions of the stir zone.

It can be seen from Figs. 4–8 that the type of ceramic particle does not play a major role to direct the nature of dispersion in the composite. All the ceramic particles considered in this research work mixed well with the plasticized aluminum and produced the composite. This can be attributed to the nature of the FSP process, which produces the composite in solid state without melting the aluminum alloy. Neither the density gradient nor the wettability between the type of ceramic particle and the aluminum causes inhomogeneous microstructure. Singla et al. [28] produced AA6061/SiC and AA6061/Al_2O_3 AMCs using stir casting and found that the dispersion of SiC particles was not similar to the dispersion of Al_2O_3 particles. The dispersion of SiC particles was homogenous while severe agglomerations of Al_2O_3 particles were observed. Mazaheri et al. [7] developed Al/TiC and Al/B_4C AMCs using stir casting and observed that the density gradient between the aluminum and the ceramic particle played a crucial role in the dispersion of particles. They concluded that it is difficult to obtain desirable dispersion of various ceramic particles using same set of process parameters. Therefore, it is difficult to produce AMCs reinforced with various ceramic particles by applying stir casting technique under a set of similar process parameters. The density gradient moves the ceramic particle either to float or sink while poor wettability causes the rejection of particles from the aluminum melt. FSP process is suitable and capable of producing AMCs reinforced with various ceramic particles.

Table 2
Properties of AA6082 aluminum matrix composites.

Material	Grain size (μm)	Microhardness (VHN)	UTS (MPa)
AA6082	39.4	62	254
AA6082/SiC AMC	6.2	102	286
AA6082/Al_2O_3 AMC	4.8	106	297
AA6082/TiC AMC	5.2	120	326
AA6082/B_4C AMC	5.3	115	315
AA6082/WC CMC	6.1	98	283

The EBSD images of AA6082 AMCs reinforced with various ceramic particles and the aluminum matrix are depicted in Fig. 9 and the quantitative values of grain size are furnished in Table 2. The aluminum matrix shows elongated grains due to the rolling process. All the AA6082 AMCs exhibit fine and equiaxed grains. The generation of fine grain structure can be explained using the following factors. FSP results in dynamic recrystallization due to intense plastic deformation since aluminum is a high stacking fault energy material. A rearrangement of dislocations into sub-grain boundaries by dynamic recovery takes place [29]. The severe plastic strain rate causes grain refinement. The driving force is

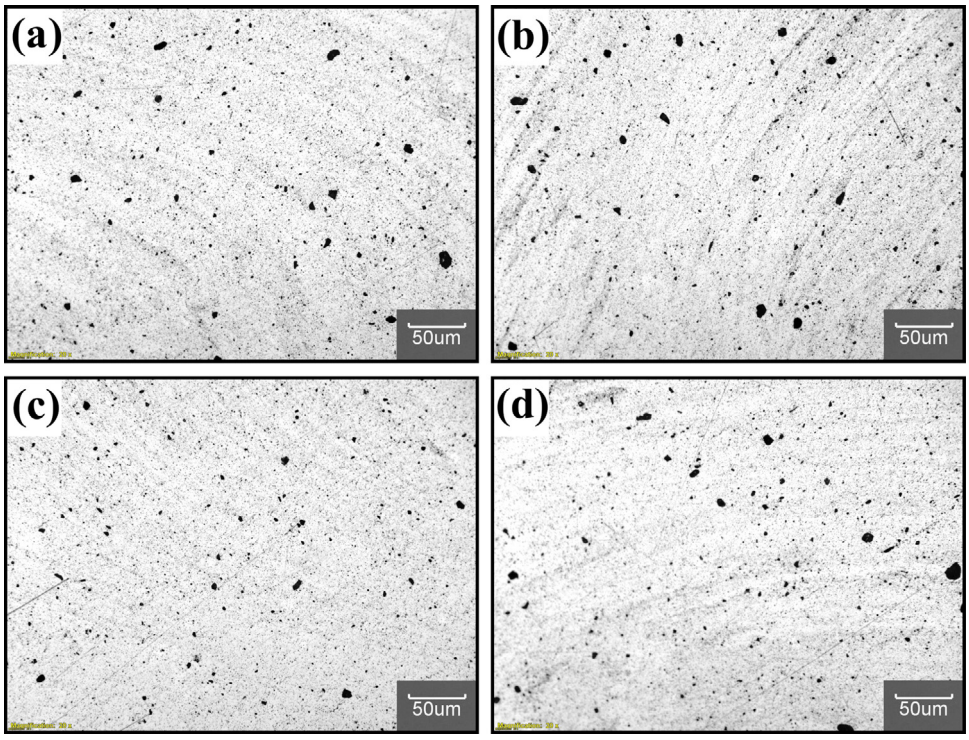

Fig. 5. Optical photomicrograph of AA6082/Al_2O_3 AMCs observed at various locations within the stir zone; (a) near advancing side, (b) near retreading side; (c) center and (d) bottom.

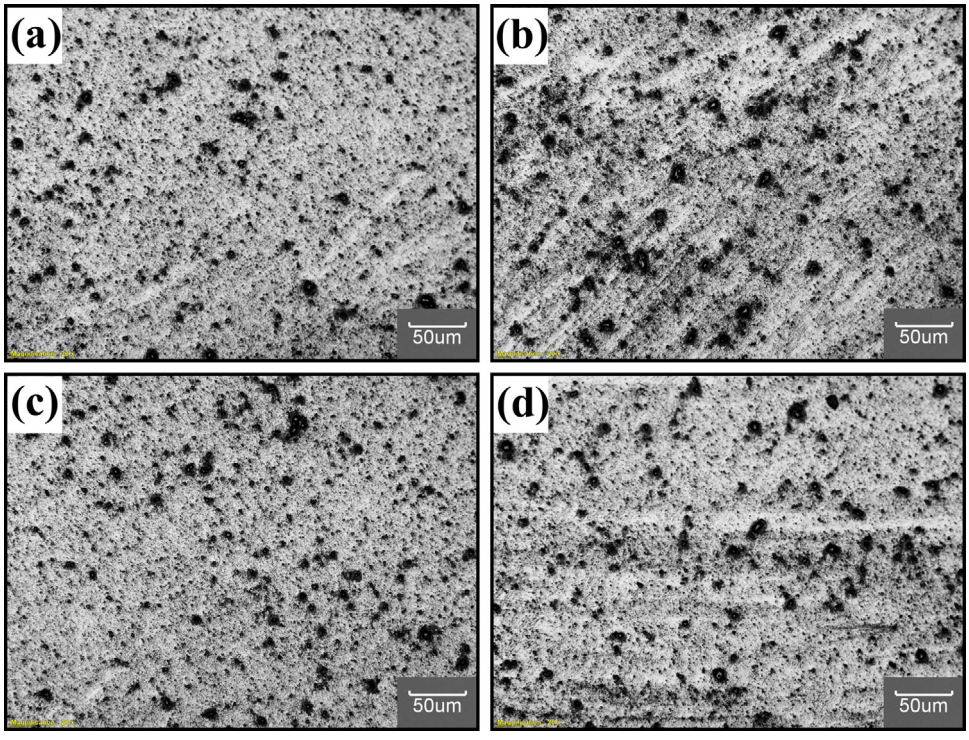

Fig. 6. Optical photomicrograph of AA6082/TiC AMCs observed at various locations within the stir zone; (a) near advancing side, (b) near retreading side; (c) center and (d) bottom.

the increased dislocation density that resulted from the applied strain, which hinders grain growth [30]. As a result, more new grains nucleate at the moving boundaries. Secondly, the ceramic particles have a tendency to pin the movement of the grain boundaries and hold up the grain growth caused by dynamic recrystallization. A growing grain boundary encounters several obstacles in its movement due to homogeneous dispersion of reinforcement particles. Thirdly, the variation in deformation of hard reinforcement particles and soft aluminum matrix during plastic deformation assists to fragment the grains. This creates finer grains.

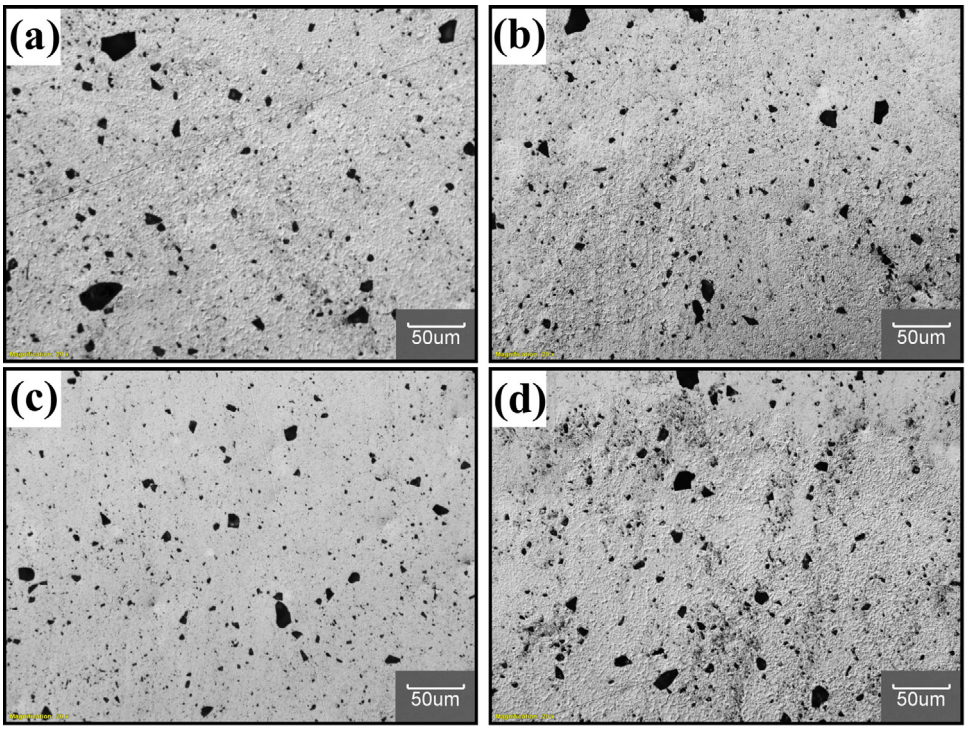

Fig. 7. Optical photomicrograph of AA6082/B_4C AMCs observed at various locations within the stir zone; (a) near advancing side, (b) near retreading side; (c) center and (d) bottom.

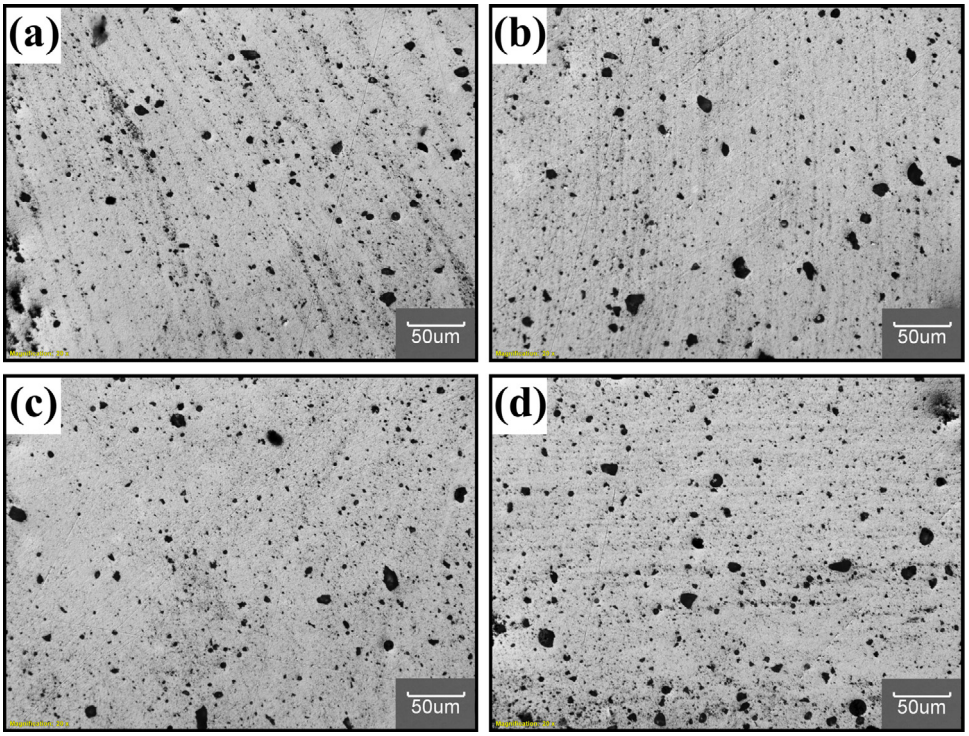

Fig. 8. Optical photomicrograph of AA6082/WC AMCs observed at various locations within the stir zone; (a) near advancing side, (b) near retreading side; (c) center and (d) bottom.

The variation in grain size among the various AA6082 AMCs is insignificant. This leads to a conclusion that the type of ceramic particle is not crucial for grain refinement. All the ceramic particles contributed to grain refinement by one or two mechanisms as discussed above.

3.2. Microhardness and tensile strength of AA6082 AMCs

The microhardness and UTS of AA6082 AMCs reinforced with various ceramic particles are given in Table 2. The microhardness and UTS of as-received AA6082 were 62 HV and 254 MPa,

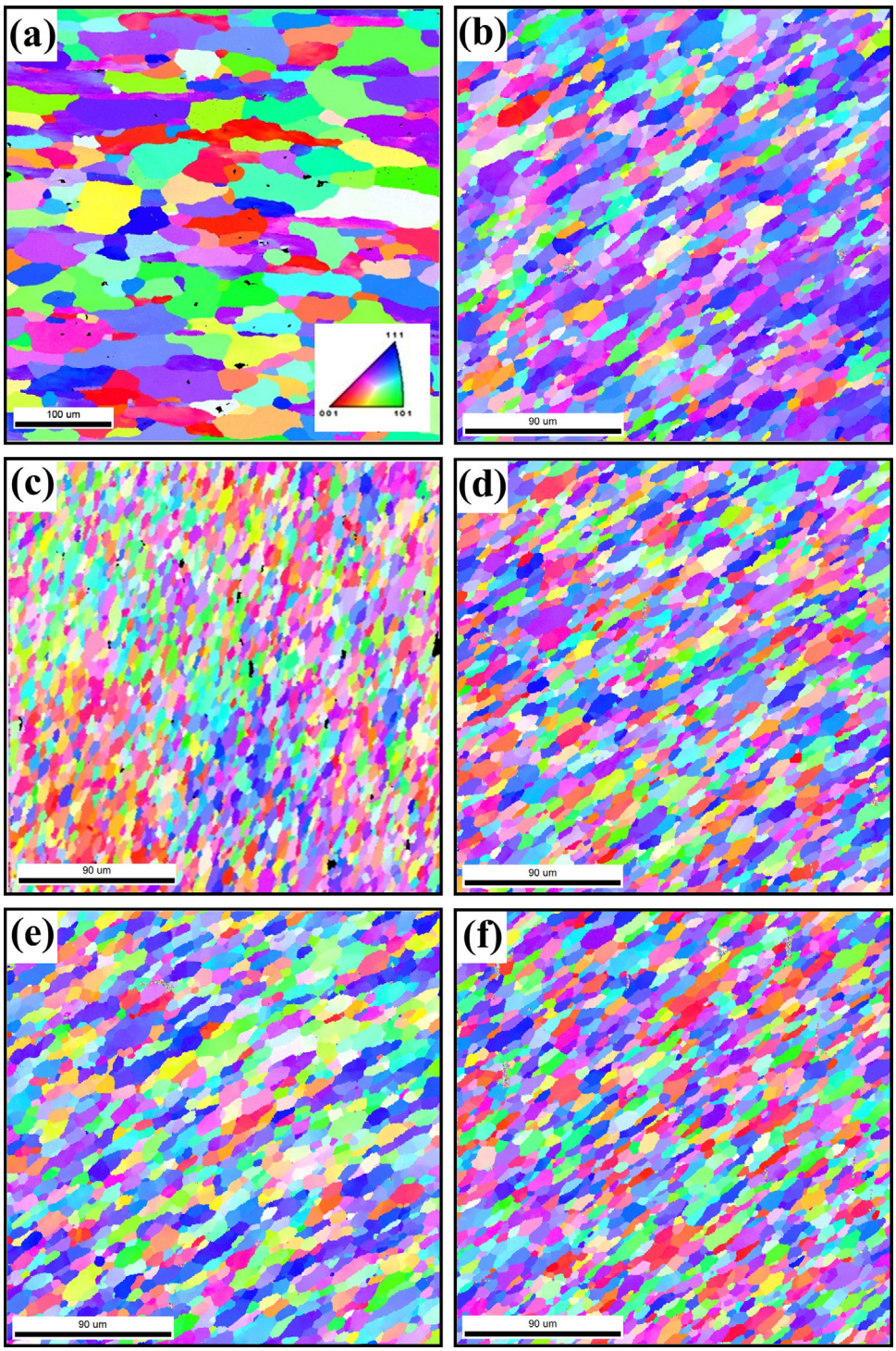

Fig. 9. EBSD (IPF + grain boundary) map of AA6082 AMCs reinforced with (a) no particle (i.e. AA6082), (b) SiC, (c) Al_2O_3, (d) TiC, (e) B_4C and (f) WC.

respectively. The incorporation of various ceramic particles improved the mirohardness and UTS. AA6082/TiC AMC exhibited higher microhardness and UTS under the experimental conditions applied in this research work. The various AMCs are strengthened by the different ceramic particles. The mechanical properties such as microhardness and UTS improved owing to the changes that took place in the microstructure. The possible strengthening mechanisms are elaborated as follows. The hardness of ceramic particles is very high to that of aluminum matrix. The dispersion of ceramic particles as a hard phase in the aluminum matrix results in strengthening. According to Hall–Petch relationship, the grain size influences the mechanical properties of metallic materials. The grain size of AA6082 AMCs is smaller to that of the AA6082 aluminum matrix due to grain refinement. The fine grains help to improve the mechanical properties. Thirdly, the variation in thermal contraction between the aluminum matrix and the ceramic particles produces quench hardening effect. Further, the homogenous dispersion of ceramic particles all over the aluminum matrix provides Orowan strengthening [31].

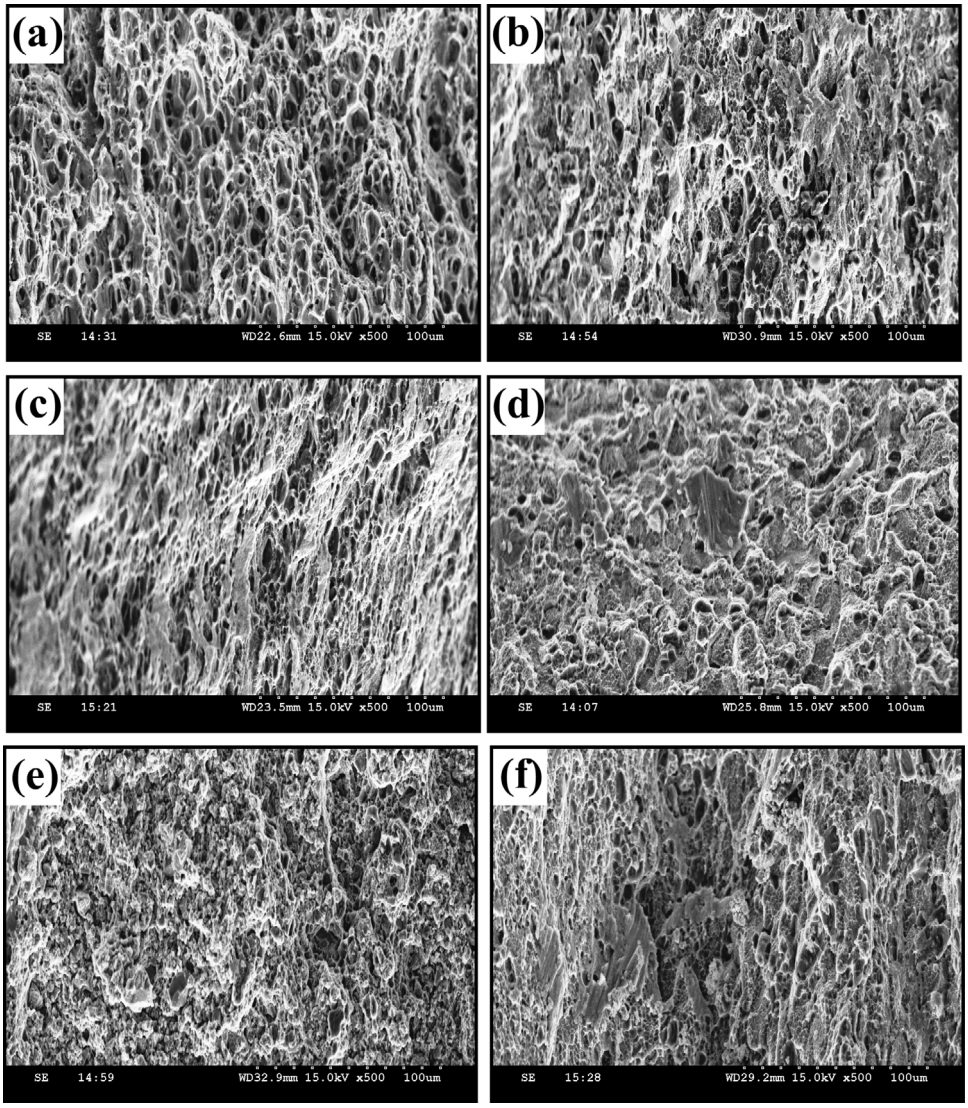

Fig. 10. Fractographs of AA6082 AMCs reinforced with (a) no particle (i.e. AA6082), (b) SiC, (c) Al_2O_3, (d) TiC, (e) B_4C and (f) WC.

The hardness of SiC, Al_2O_3, TiC, B_4C and WC are respectively 2480 HK, 2100 HK, 2470 HK, 2750 HK and 1880 HK. Nevertheless, AA6082/TiC AMC showed higher mirohardness and UTS. The variations in microhardness and UTS are respectively within 19% and 13%. There are several factors that govern the mechanical properties of AMCs including size, shape, volume fraction, nature of distribution of ceramic particles [32,33]. All types of ceramic particles displayed homogeneous dispersion in the aluminum matrix for a selected constant volume fraction. There are no clusters or porosities present in considerable quantity. Al_2O_3 particle is smaller in size compared to other ceramic particles studied in this work. But, the hardness of Al_2O_3 is lower to that of TiC. The hardness of B_4C is higher compared to all other ceramic particles. However, B_4C particles display (Fig. 2d and 3d) sharp edges in the AMC which may act as stress raiser during tensile loading. SiC particles are bigger in size and having sharp edges. The fine size and spherical morphology of the TiC particles could be the possible reason for higher mechanical properties of AA6082/TiC AMC.

The fracture surfaces of AA6082 AMCs reinforced with various ceramic particles and the aluminum matrix are presented in Fig. 10. The fracture surface of the aluminum matrix is covered with a uniform dispersion of large size void. It indicated large amount of material flow before failure. The fracture mode observed is ductile. The fracture surface of the AA6082 AMCs reveals a bimodal dispersion of large and small size of dimples. This is a typical fracture surface of AMCs, which have well-bonded reinforcement particles. Large dimples are formed wherever ceramic particles are present. Small dimples arise due to the ductile failure of the aluminum matrix. The bimodal dispersion of dimples indicates that the failure is brittle macroscopically and ductile microscopically. The presence of ceramic particles restricts the flow of aluminum matrix during tensile loading. Fracture surfaces confirm that the applied load was effectively transferred to the ceramic particles due to good interfacial bonding.

4. Conclusion

AA6082/X (X = SiC, Al_2O_3, TiC, B_4C and WC) AMCs were successfully produced using FSP. The microstructure, microhardness and tensile strength were evaluated. The following conclusions are derived from the present work.

- The variation in grain size, microhardness and UTS was within a short range. Nevertheless, AA6082/TiC AMC displayed better hardness and UTS compared to other AMCs produced in this work under the same set of experimental conditions.

- The dispersion of the ceramic particles in the AA6082 AMCs was independent of the location within the stir zone. The dispersion was homogeneous and unaffected by the type of ceramic particle used.
- SiC, TiC, B_4C and WC particles encountered fragmentation during FSP due to severe plastic deformation and interaction with the rotating tool. The fragmented debris also mixed well with the plasticized aluminum and dispersed homogeneously in the AMC. Al_2O_3 particle did not suffer fragmentation due to its smaller size.
- There was no interfacial reaction between aluminum and any type of ceramic particle and good interfacial bonding was observed.
- All types of ceramic particles enhanced the UTS of aluminum alloy AA6082 and influenced the fracture mode. The fracture mode shifted from ductile to brittle.
- FSP is a suitable processing method to produce AMCs reinforced with various kinds of ceramic particles with acceptable properties.

Acknowledgements

The author is grateful to Welding Research Cell at Coimbatore Institute of Technology, OIM and Texture Lab at Indian Institute of Technology Bombay and Metmech Engineers Research Lab at Chennai for providing the facilities to carry out this investigation.

References

[1] P. Sharma, S. Sharma and D. Khanduja, J. Asian Ceram. Soc., 3, 240–244 (2015).
[2] L.J. Zhang, F. Qiu, J.G. Wang and Q.C. Jiang, Mater. Sci. Eng. A, 626, 338–341 (2015).
[3] H.S. Chen, W.X. Wang, Y.L. Li, P. Zhang, H.H. Nie and Q.C. Wu, J. Alloys Compd., 632, 23–29 (2015).
[4] M. Rosso, J. Mater. Process. Technol., 175, 364–375 (2006).
[5] M. Rahimian, N. Ehsani, N. Parvin and H.R. Baharvandi, J. Mater. Process. Technol., 209, 5387–5393 (2009).
[6] H.S. Chen, W.X. Wang, H.H. Nie, Y.L. Li, Q.C. Wu and P. Zhang, Acta Metall. Sin., 28, 1214–1221 (2015).
[7] Y. Mazaheri, M. Meratian, R. Emadi and A.R. Najarian, Mater. Sci. Eng. A, 560, 278–287 (2013).
[8] B.S. Yigezu, P.K. Jha and M.M. Mahapatra, Mater. Manuf. Processes, 28, 969–979 (2013).
[9] P. Sharmaa, S. Sharma and D. Khanduja, J. Asian Ceram. Soc., 3, 352–359 (2015).
[10] Z.Y. Ma, Metall. Mater. Trans. A, 39, 642–658 (2008).
[11] Y.X. Gan, D. Solomon and M. Reinbolt, Materials, 3, 329–350 (2010).
[12] H.S. Arora, H. Singh and B.K. Dhindaw, Int. J. Adv. Manuf. Technol., 61, 1043–1055 (2012).
[13] V. Sharma, U. Prakash and B.V. Manoj Kumar, J. Mater. Process. Technol., 224, 117–134 (2015).
[14] S. Shahraki, S. Khorasani, R.A. Behnagh, Y. Fotouhi and H. Bisadi, Metall. Mater. Trans. B, 44, 1546–1553 (2013).
[15] M.A. Moghaddas and S.F.K. Bozorg, Mater. Sci. Eng. A, 559, 187–193 (2013).
[16] G.L. You, N.J. Ho and P.W. Kao, Mater. Charact., 80, 1–8 (2013).
[17] M. Bahrami, M.K.B. Givi, K. Dehghani and N. Parvin, Mater. Des., 53, 519–527 (2014).
[18] Y. Mazaheri, F. Karimzadeh and M.H. Enayati, Metall. Mater. Trans. A, 45, 2250–2259 (2014).
[19] F. Khodabakhshi, A. Simchi, A.H. Kokabi, A.P. Gerlich and M. Nosko, Mater. Des., 63, 30–41 (2014).
[20] A. Thangarasu, N. Murugan, I. Dinaharan and S.J. Vijay, Arch. Civ. Mech. Eng., 15, 324–334 (2015).
[21] Y. Zhao, X. Huang, Q. Li, J. Huang and K. Yan, Int. J. Adv. Manuf. Technol., 78, 1437–1443 (2015).
[22] R. Hashemi and G. Hussain, Wear, 324–325, 45–54 (2015).
[23] C.J. Lee, J.C. Huang and P.J. Hsieh, Scr. Mater., 54, 1415–1420 (2006).
[24] A. Devaraju, A. Kumar and B. Kotiveerachari, Mater. Des., 45, 576–585 (2013).
[25] O.S. Salih, H. Ou, W. Sun and D.G. McCartney, Mater. Des., 86, 61–71 (2015).
[26] E.R.I. Mahmoud, K. Ikeuchi and M. Takahashi, Sci. Technol. Weld. Join., 13, 607–618 (2008).
[27] D.K. Lim, T. Shibayanagi and A.P. Gerlich, Mater. Sci. Eng. A, 507, 194–199 (2009).
[28] Y.K. Singla, R. Chhibber, H. Bansal and A. Kalra, JOM, 67, 2160–2169 (2015).
[29] R. Bauri, D. Yadav, C.N.S. Kumar and B. Balaji, Mater. Sci. Eng. A, 620, 67–75 (2015).
[30] M. Narimani, B. Lotfi and Z. Sadeghian, Surf. Coat. Technol., 285, 1–10 (2016).
[31] Z. Zhang and D.L. Chen, Mater. Sci. Eng. A, 483–484, 148–152 (2008).
[32] A.P. Sannino and H.J. Rack, Wear, 189, 1–19 (1995).
[33] S. Sahraeinejad, H. Izadi, M. Haghshenas and A.P. Gerlich, Mater. Sci. Eng. A, 626, 505–513 (2015).